



HAL
open science

Playing with Magnetic Anisotropy in Hexacoordinated Mononuclear Ni(II) Complexes, An Interplay Between Symmetry and Geometry

Nicolas Suaud, Guillaume Rogez, Jean-Noël Rebilly, Mohammed-Amine Bouammali, Nathalie Guihéry, Anne-Laure Barra, Talal Mallah

► **To cite this version:**

Nicolas Suaud, Guillaume Rogez, Jean-Noël Rebilly, Mohammed-Amine Bouammali, Nathalie Guihéry, et al.. Playing with Magnetic Anisotropy in Hexacoordinated Mononuclear Ni(II) Complexes, An Interplay Between Symmetry and Geometry. *Applied Magnetic Resonance*, 2020, 51, pp.1215-1231. 10.1007/s00723-020-01228-8 . hal-02996042

HAL Id: hal-02996042

<https://hal.science/hal-02996042>

Submitted on 9 Nov 2020

HAL is a multi-disciplinary open access archive for the deposit and dissemination of scientific research documents, whether they are published or not. The documents may come from teaching and research institutions in France or abroad, or from public or private research centers.

L'archive ouverte pluridisciplinaire **HAL**, est destinée au dépôt et à la diffusion de documents scientifiques de niveau recherche, publiés ou non, émanant des établissements d'enseignement et de recherche français ou étrangers, des laboratoires publics ou privés.

Playing with magnetic anisotropy in hexacoordinated mononuclear Ni(II) complexes, an interplay between symmetry and geometry

Nicolas Suaud,^a Guillaume Rogez,^b Jean-Noël Rebilly,^c Mohammed-Amine Bouammali,^a Nathalie Guihéry,^{*a} Anne-Laure Barra,^{*d} and Talal Mallah^{*c}

^a *Laboratoire de Chimie et Physique Quantiques, Université de Toulouse III, 118, route de Narbonne, 31062 Toulouse, France. E-mail: nathalie.guihery@irsamc.ups-tlse.fr*

^b *IPCMS-GMI, UMR CNRS 7504, 23, rue du Loess, B.P. 43, 67034 Strasbourg Cedex 2, France.*

^c *Institut de Chimie Moléculaire et des Matériaux d'Orsay, CNRS, Université Paris-Saclay, 91405 Orsay, France. E-mail: talal.mallah@universite-paris-saclay.fr, ORCID: 0000-0002-9311-3463.*

^d *Laboratoire National des Champs Magnétiques Intenses, UPR CNRS 3228, Univ. Grenoble Alpes, 25, avenue des Martyrs, B.P. 166, 38042 Grenoble Cedex 9, France. E-mail: anne-laure.barra@lncmi.cnrs.fr*

The magnetic anisotropy parameters of a hexacoordinate trigonally elongated Ni(II) complex with symmetry close to D_{3d} are measured using field-dependent magnetization and High-Field and High-Frequency EPR spectroscopy ($D = +2.95 \text{ cm}^{-1}$, $|E/D| = 0.08$ from EPR). Wavefunction based theoretical calculations reproduce fairly well the EPR experimental data and allows analysing the origin of the magnetic anisotropy of the complex. Calculations on model complexes allows getting insight into the origin of the large increase in the axial magnetic anisotropy (D) when the complex is brought to a prismatic geometry with a symmetry close to D_{3h} .

1. Introduction

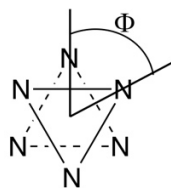
The majority of hexacoordinate Ni(II) complexes (d^8 configuration and $S = 1$) have an octahedral geometry that is usually distorted and present a zero-field splitting (ZFS) of the M_S sub-levels (± 1 and 0) characterized by two parameters D (axial) and E (rhombic). ZFS originates from the simultaneous effects of geometrical distortions from O_h symmetry and spin-orbit coupling. In the ideal case of O_h symmetry point group, the three components (\hat{L}_x , \hat{L}_y and \hat{L}_z) of the angular orbital momentum belong to the same irreducible representation (IRREP) T_{1g} and the effect of the spin-orbit coupling (SOC) is the same in the three directions of space preventing the occurrence of ZFS. In the presence of a weak axial distortion, a weak ZFS occurs stabilizing either the $M_S = \pm 1$ levels (negative D value corresponding to an easy axis of magnetization, see eq. 1) or the $M_S = 0$ (positive D value corresponding to an easy plane of magnetization). A deviation from axiality leads to a lift of degeneracy of the $M_S = \pm 1$ levels by $2E$ where E is the rhombic ZFS parameter based on the following spin Hamiltonian:

$$H_{ZFS} = D[\hat{S}_z^2 - S(S + 1)/3] + E(\hat{S}_x^2 - \hat{S}_y^2) \quad (1)$$

with \hat{S}_i ($i = x, y, z$) the components of the spin operator.

For an orbitally non-degenerate ground state as for octahedral geometry, the effect of SOC can be taken into account by admixture between the ground and the excited states. Using second order perturbation theory, contributions of excited states to the ZFS parameters are inversely proportional to their energy difference with the ground state. The magnitude of $|D|$ is therefore inversely proportional to the energy difference between ground and excited states coupled through SOC. For a given axial symmetry, the sign of D , that determines the nature of the magnetization (easy axis or easy plane) depends, therefore, on the nature (compression or elongation along the main symmetry axis) of the distortion.[1,2] Combining these two arguments, it is possible to "control" both the nature and magnitude of ZFS by chemical means playing on the geometry, the symmetry of the complexes and the nature of the atoms coordinated to the metal ion, as it has already been investigated by several groups.[3-12]

In order to get insight in the interplay between geometry and symmetry, we investigated, using High Field-High Frequency Electron Paramagnetic Resonance (HF-HFEPR) spectroscopy and *ab initio* calculations, the ZFS of an already reported octahedral Ni(II) complex of formula $[\text{Ni}(\text{tacn})_2]^{2+}$ where tacn is the triazacyclononane macrocycle bearing three amine donor atoms.[13,14] The two tacn ligands impose a trigonal distortion from the octahedron leading to a complex with a symmetry close to D_{3d} for the coordination sphere of Ni(II). We carried out a theoretical study on $[\text{Ni}(\text{tacn})_2]^{2+}$ and on model complexes obtained from reducing the twist angle Φ (Scheme 1) from 60° to 0° in order to examine the effect of crossing from D_{3d} to D_{3h} symmetry on the nature and the magnitude of the axial ZFS parameter D .



Scheme 1.

2. Experimental and methods

2.1 Synthesis and X-ray

The $[\text{Ni}(\text{tacn})_2](\text{ClO}_4)_2$ (**1**) compound was prepared as already described and the crystal structure was checked to be identical to the reported one.[13,14]

2.2 Magnetic measurements

Magnetization measurements were performed on a Quantum Design MPMS5 SQUID magnetometer. The powder obtained from ground crystals of **1** was blocked in parafilm to avoid any orientation of the sample. Data was corrected from parafilm contribution and diamagnetism was estimated from Pascal constants.

An isotropic g -factor was considered to reduce the variable parameters during the fit procedure.

2.3 HF-HF EPR

HF-HF EPR measurements were performed with a multi-frequency spectrometer operating in a single-pass configuration.[15] A 95 GHz Gunn oscillator (Radiometer Physics GmbH) is multiplied by a doubler or a tripler to obtain 190 or 285 GHz, respectively. The detection is performed with a hot electron InSb bolometer (QMC Instruments). The exciting light is propagated with oversized waveguides all over the optical path. The main magnetic field is supplied by a 12 T superconducting magnet equipped with a VTI (Cryogenics). The measurements were done on powdered samples pressed into pellets in order to limit torquing effects.

Calculated spectra were obtained in two steps: a fitting of the identified resonance positions[16] to obtain the parameters driving the spin Hamiltonian (eq. 2) and a calculation of the spectra with the SIM program,[17] which diagonalizes the resulting spin Hamiltonian. Both programs were developed by H. Weihe (Univ. of Copenhagen).

2.4 Theoretical calculations

In a first step, a DFT geometry optimization (PBE functional) of the hydrogen only atoms of a single complex embedded in a fix environment of its 8 nearest-neighbours ClO_4^- anions was performed, taking the position of the non-hydrogen atoms from the crystallographic structure. Then, the D and E parameters were evaluated following the procedure developed in ref.[18] and applied with success for a series of complexes among many others.[9,12,19-21] A State Average CASSCF (Complete Active Space Self Consistent Field) was performed;

then, the dynamical correlation is added by NEVPT2 method in its strongly contracted scheme, without frozen core.[22-24]. Finally, the Spin-Orbit (SO) coupling was accounted for by RASSISO calculations.[25] The Complete Active Space (CAS) is composed of the five mainly-3d orbitals of the Ni ion and the 8 associated electrons, *i.e.* CAS(8,5). The averaging of the molecular orbitals CASSCF optimization (MO) was done over all the 10 triplet and 15 singlet spin states generated by the CAS(8,5). The SO coupling was considered between all these states, the spin-free energy (diagonal elements of the SO matrix) being evaluated at the NEVPT2 level.

For the model complexes, the calculations were made using the coordinate of the structures obtained from changing the twist angle Φ (Scheme 1) from 60° (for **1**) to 45 , 30 , 15 and 0° .

For DFT geometry optimization, 5s3p2d1f for the Ni center, 4s3p1d for Cl, 3s2p1d for O, N and C atoms and 2s1p for H atoms sets of atomic orbitals (OA) were used. In CASSCF, NEVPT2 and RASSISO, DKH-def2-QZVPP basis sets were used for Ni and N atoms (14s10p5d4f2g and 8s4p3d2f1g respectively), DKH-def2-TZVP basis sets for C atoms (6s3p2d1f) and DKH-def2-SVP basis sets for H atoms (2s1p). The AUTOAUX feature[26] was used to automatically generate auxiliary basis sets for the resolution of identity approximation (RI-JK),[27] which helps speed up the calculation. Scalar relativistic effects were accounted for using the second-order scalar relativistic Douglas Kroll Hess (DKH2) Hamiltonian formalism.[28] All calculations were performed using the ORCA 4.2.1 quantum chemistry package.[29]

3. Results and discussion

The crystal structure of the Ni(tacn)²⁺ cation (Fig. 1) shows that Ni is hexacoordinated and located on an inversion center. The Ni-N bond lengths have an average value of 2.115 Å and their maximum difference is less than 0.02 Å. The set of bite angles imposed by the macrocycle has an average value of the NNiN angles of 81.7° with a difference of less than 0.4° . The angles between the pseudo C_3 axis of the complex and the Ni-N bonds are almost the same and are equal to 49° , while this angle is 54.7° in the case of a regular octahedron. The twist angle Φ (Scheme 1) is equal to 60° . From the geometrical point of view, the complex can be considered as an octahedron with an elongated trigonal distortion along a pseudo three-fold symmetry axis, resulting in a close to D_{3d} symmetry.

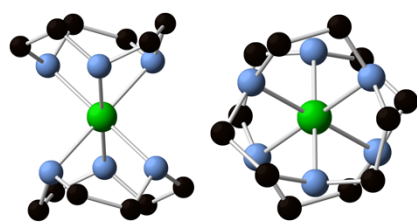


Figure 1. View of the molecular structure of **1** with the pseudo C_3 axis within (left) and perpendicular (right) to the plane. The H atoms were removed for clarity. C(black), N(blue) and Ni(green).

Magnetization vs field measurements between 0 and 5.5 Tesla at different temperatures were performed using a SQUID magnetometer. The $M = f(B/T)$ plots for $T = 2, 3, 4$ and 6 K are not superimposable, which is a signature of the presence of ZFS within the $S = 1$ state and therefore magnetic anisotropy (Fig. 2). The experimental data were fitted by exact diagonalisation of the energy matrices corresponding to the spin Hamiltonian:

$$H = \mu_B \mathbf{S}[\mathbf{g}]\mathbf{B} + H_{ZFS} \quad (2)$$

using a home made software. It was not possible to determine unambiguously the sign of the axial parameter D from this experiment. Actually, two different sets of parameters were obtained with almost identical agreement factors, the first one with $D > 0$ ($D = +2.92 \text{ cm}^{-1}$, $|E/D| = 0.12$, $g = 2.12$ with $R = 5.2 \times 10^{-5}$) and the other one with $D < 0$ ($D = -3.08 \text{ cm}^{-1}$, $|E/D| = 0.26$, $g = 2.13$ with $R = 3.7 \times 10^{-5}$). This analysis of the magnetization data leads to the conclusion that $|D|$ is around 3 cm^{-1} and $|E/D|$ is in the range $0.1-0.3$.

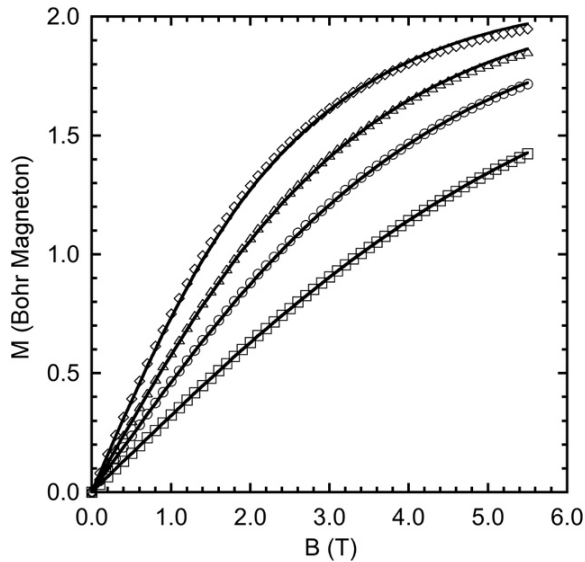


Figure 2. Magnetization (top) and reduced magnetization (right) plots for **1** at $T = 2(\diamond)$, $3(\triangle)$, $4(\circ)$ and $6(\square)$ K, the lines correspond to the best fit (bottom) (see text).

In order to determine the sign of the axial ZFS parameter D , we performed a High-Field and High-Frequency EPR (HF-HFEPR) study at two different frequencies, namely 190 GHz and 285 GHz, and several temperatures. For such frequencies, large depopulation effects take place among the M_s levels at helium temperature which allow one to obtain the sign of D . Actually, for $D > 0$, one expects that the intensity of the low field parallel transition (labeled z1 on figures 3 and 4) decreases on decreasing the temperature meanwhile the intensity of z2 increases, whereas the opposite evolution is expected for the transitions associated to the x and y orientations. For $D < 0$, the temperature dependence of the transitions will be opposite. The powder spectra collected at 190 and 285 GHz and

at 5 and 15 K are displayed in figures 3 and 4. These spectra are consistent with those expected for a spin-triplet when the ZFS is comparable with or smaller than the Zeeman interaction.[2] The main feature is the very intense half-field transition (at 2.7 T and 4.5 T for 190 GHz and 285 GHz resp.), the others being weaker. The classical pattern of the spectra allows assigning the signals for the principal orientations (z, y and x).

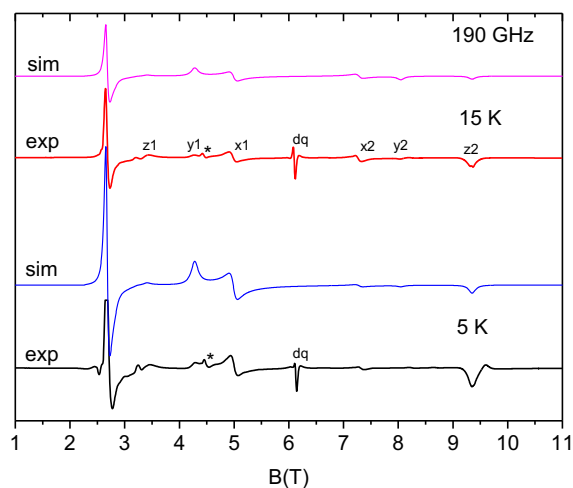


Figure 3. Powder HF-HFEPR spectra of **1** at 190 GHz at 5 K (lower traces) and 15 K (higher traces), experimental (exp) and simulated (sim) with the parameters indicated in the text. The asterisk indicates a signal arising from a higher frequency harmonic (285 GHz).

When going from 5 to 15 K, the z1 transition increases whereas the z2 decreases (at 285 GHz the z2 transition is not visible as it is expected at a field higher than 12 T, the maximum field of the magnet). This means that z1 corresponds to the $M_s = 0 \rightarrow +1$ transition and z2 to the $M_s = -1 \rightarrow 0$ one, a clear signature that $D > 0$.

The fit of the resonance positions[16] gave the following set of parameters: $D = +2.95(3) \text{ cm}^{-1}$, $E = 0.24(1) \text{ cm}^{-1}$ ($E/D = 0.08$), $g_x = 2.14(1)$, $g_y = 2.15(1)$, $g_z = 2.13(1)$ and $g_{av} = (g_x + g_y + g_z)/3 = 2.14$ and allowed obtaining very nice simulations of the spectra (Fig. 3 and 4).[17] The values obtained are also in good agreement with the results of the magnetization study (considering the $D > 0$ option). They confirm that the complex possesses a moderate and rather axial ZFS.

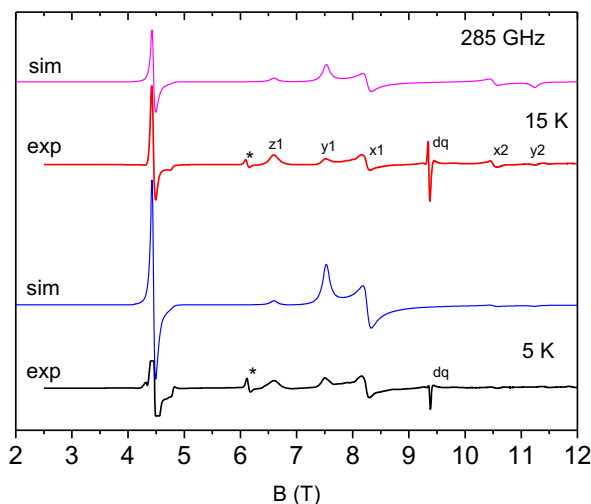


Figure 4. Powder HF-HFEPR spectra of **1** at 285 GHz at 5 K (lower traces) and 15 K (higher traces), experimental (exp) and simulated (sim) with the parameters indicated in the text. At 5 K, the half-field signal (exp) was truncated during the measurement. The asterisk indicates a signal arising from a higher frequency harmonic (380 GHz).

Besides the half-field transition and the $\Delta M_S = \pm 1$ ones, another signal is observed, labeled *dq* on the experimental spectra. It is assigned to the double quantum transition as it presents the characteristics expected for such transition and found where it is expected:[30,31] $B_{dq}^{190} = 6.10$ T and $B_{dq}^{285} = 9.36$ T using equation 3:

$$B_{dq} = \frac{g_e}{g_{av}} \sqrt{B_0^2 - \frac{D^2}{3} - E'^2} \quad (3)$$

where B_0 is the resonance field of the free electron, g_e its g factor, $g_{av} = (g_x + g_y + g_z)/3$, $D = \frac{D'}{\mu_B g_e}$ and $E = \frac{E'}{\mu_B g_e}$. [30]

Wave-function based *ab initio* calculations allow getting insight into the different electronic parameters that govern both the nature and magnitude of ZFS. Using model complexes allows one to examine the effect of structural changes on the magnitude of the ZFS parameters and to establish magneto-structural correlations.

For **1**, calculations using the NEVPT2 electronic energies, (see Methods section) gives $D = 4.3$ cm^{-1} and $E = 0.2$ cm^{-1} ($E/D = 0.05$) with $g_x = 2.18$, $g_y = 2.18$, and $g_z = 2.15$. Given the rather weak ZFS parameters, the agreement with the experimental values determined from HF-HFEPR can be considered as very good. In particular, theoretical calculations give the right sign for the axial parameter D , which justifies their use to perform the analysis made below. In O_h symmetry point group and before considering the effect of SOC, the ten triplet states of the d^8 configuration gather in four blocks: the ground (${}^3A_{2g}$) and three excited (${}^3T_{2g}$, ${}^3T_{1g}$ and ${}^3T_{1g}$) states. Reducing the symmetry to D_{3d} lifts the three-fold orbital degeneracy of the excited states, which results in three sets of two states: one non-degenerate (either ${}^3A_{1g}$ or ${}^3A_{2g}$) and one doubly degenerate (3E_g). This is what we observe for **1** as depicted in Figure 5 showing that the hexacoordinate complex behaves electronically as a trigonal

one. Because the symmetry is, actually, not exactly D_{3d} , the orbital degeneracy of the 3E_g states is slightly lifted with an energy difference of approximately 100 cm^{-1} , while the energy difference between the ${}^3A_{1g(2g)}$ and the pseudo 3E_g states is as large as 2000 cm^{-1} . In summary, one can reasonably consider that the spectrum of **1** is very close to that of a D_{3d} complex.

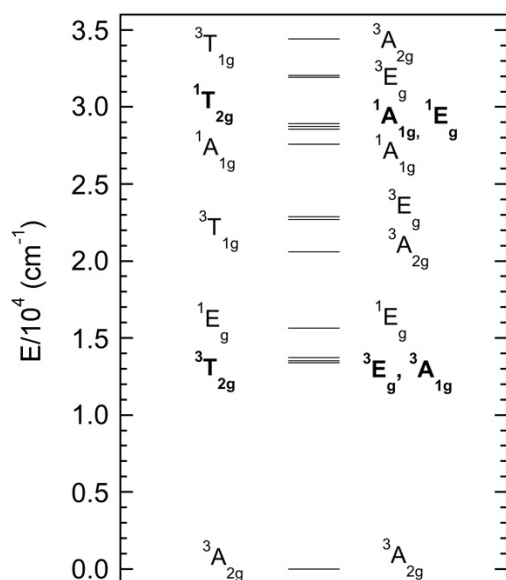


Figure 5. NEVPT2 energy of the lowest states (excluding the highest singlets) with the IRREPs in D_{3d} symmetry point group (right) and the IRREPs with which they correlate in O_h symmetry point group (left); the excited states that contribute to D are in bold.

After SOC, the three-fold spin degeneracy of the triplet ground state is lifted leading to three levels with a small energy difference described by the D and E parameters. In order to rationalize the magnitude and nature (either negative or positive) of the axial ZFS parameter D , we examined the contribution to D of each excited state. Among the nine excited triplet states, only the three first ones couple to the ground state and contribute quantitatively to D by 13.45 , 7.33 and -15.91 cm^{-1} (Table 1). The six remaining triplet states that are higher in energy (issued from the two ${}^3T_{1g}$ in O_h symmetry) have contributions close to zero. The origin of this behavior is due to the fact that D_{3d} is a sub-group of O_h and the SOC's between ground and excited states can be related to those observed in O_h . For O_h symmetry, it has already been shown that only the lower ${}^3T_{2g}$ state couples to the ground state via SOC while the two ${}^3T_{1g}$ states do not.[2] Therefore, as the first three triplets of **1** correlate with ${}^3T_{2g}$ of O_h and because they are no more degenerate in the almost D_{3d} symmetry of **1**, they contribute to D , while the higher six triplets that correlate with ${}^3T_{1g}$ do not. Therefore, the relatively small D value is due to the presence of negative and positive contributions that when added lead to a small value. Actually, for a perfect octahedron, they add to exactly

zero as stated above) and from the structural point of view, the slight deviation from the octahedron in **1** is responsible of an average value of the different contributions that is not far from zero, therefore, small.

Table 1. Main determinants (second column) of the wave functions of the ground and excited states that contribute to D . Doubly occupied orbitals do not appear. For simplicity, $|\overline{xz}|$ stands for the closed-shell determinant where the xz orbital is empty. Calculations are done in the magnetic axes frame. The energies (in cm^{-1}) of the states obtained at the NEVPT2 level are given in the third column while the elements of the SO-SI matrix (in cm^{-1}) and the contributions (in cm^{-1}) to D are given in the fourth and fifth columns respectively.

State ^a	Wave function composition	Energy	$\langle T0, 1 H^{SO} A^*, 1 \rangle /$ $\langle T0, 0 H^{SO} A^*, 1 \rangle =$ $\langle T0, 1 H^{SO} A^*, 0 \rangle /$ $\langle T0, 0 H^{SO} A^*, 0 \rangle$	Contribution to D
Complex 1 ($\Phi = 60^\circ$)				
$T0^b$	$0.70 yz, xz + 0.43 x^2 - y^2, xz $ $+ 0.38 yz, xy - 0.31 xy, x^2 - y^2 + \dots$	0	–	–
$T1$	$0.66 yz, x^2 - y^2 - 0.55 yz, z^2 -$ $0.36 x^2 - y^2, z^2 + 0.27 xy, z^2 + \dots$	13376	$167 i / 456 + 4.7 i / 0$	13.45
$T2$	$-0.60 yz, xy + 0.52 z^2, xz +$ $0.36 xy, xz + 0.30 x^2 - y^2, xz $ $- 0.29 xy, z^2 + \dots$	13523	$-280 i / 65 - 417 i / 0$	7.33
$T3$	$0.66 xy, xz - 0.51 x^2 - y^2, xz $ $- 0.41 yz, x^2 - y^2 - 0.31 z^2, xz + \dots$	13735	$-531 i / 113 + 225 i / 0$	-15.91
$T4$	$0.65 yz, xz - 0.50 yz, xy - 0.46 $ $x^2 - y^2, xz + 0.26 yz, x^2 - y^2 + \dots$	20581	$-0.2 i / -5.7 + 4.1 i / 0$	0.002
$S2^c$	$0.33(yz, \overline{z^2} - \overline{yz}, z^2 $ $+ 0.29(z^2, \overline{x^2 - y^2} - \overline{z^2}, x^2 - y^2 $ $- 0.25(yz, \overline{x^2 - y^2} - \overline{yz}, x^2 - y^2)$ $+ 0.25(xy, \overline{xz} - \overline{xy}, xz) + \dots$	28567	$- / 436 - 35 i / -25 i$	-6.69
$S3$	$0.34(yz, \overline{xz} - \overline{yz}, xz)$ $- 0.29(z^2, \overline{xz} - \overline{z^2}, xz)$ $- 0.29(xy, \overline{z^2} - \overline{xy}, z^2)$ $- 0.22(xz, \overline{x^2 - y^2} - \overline{xz}, x^2 - y^2 $ $- 0.22(xy, \overline{yz} - \overline{xy}, yz) + \dots$	28746	$- / -33 - 433 i / 67 i$	-6.40
$S4$	$0.52 \overline{xz} - 0.49 \overline{x^2 - y^2} $	28915	$- / 22 + 46 i / 605 i$	12.58

	$-0.48 \overline{xy} + 0.43 \overline{yz} $			
Model complex with $\Phi = 0^\circ$				
<i>T</i> 0	$0.96 yz, xz - 0.27 xy, x^2 - y^2 $	0	–	–
<i>T</i> 1	$-0.64 x^2 - y^2, xz - 0.60 yz, xy -$ $0.43 yz, x^2 - y^2 + \dots$	7487	0 / -173 +22 i / 0	4.05
<i>T</i> 2	$0.65 xy, xz - 0.64 yz, x^2 - y^2 $ $+ 0.35 yz, xy + \dots$	7534	0 / -7.2 -78 i / 0	0.81
<i>T</i> 3	$-0.54 x^2 - y^2, xz - 0.43 yz, z^2 $ $-0.42 z^2, xz - 0.40 yz, x^2 - y^2 $ $+ 0.37 xy, xz + \dots$	8186	0 / 388 + 376 i / 0	35.39
<i>T</i> 4	$-0.53 yz, xy + 0.49 xy, xz $ $+0.44 z^2, xz - 0.40 yz, z^2 + \dots$	8223	0 / 357 -400 i / 0	34.65
<i>S</i> 2	$0.47(yz, \overline{x^2 - y^2} - \overline{yz}, x^2 - y^2 $ $-0.46(xy, \overline{xz} - \overline{xy}, xz)$ $-0.25(yz, \overline{z^2} - \overline{yz}, z^2) + \dots$	20558	- / -344 - 38 i / 0	-5.82
<i>S</i> 3	$0.47(xz, \overline{x^2 - y^2} - \overline{xz}, x^2 - y^2 $ $-0.46(xy, \overline{yz} - \overline{xy}, yz)$ $+0.24(z^2, \overline{xz} - \overline{z^2}, xz) + \dots$	20582	- / -37 + 343 i / 0	-5.78
<i>S</i> 4	$0.54 \overline{xz} + 0.53 \overline{yz} $ $- 0.46 \overline{x^2 - y^2} $ $- 0.45 \overline{xy} + \dots$	21775	- / 0 / 705 i	22.82

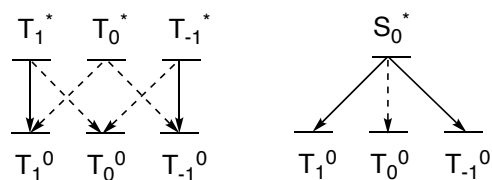
^aThe states are numbered according to their energetic order from lowest to highest. Only the singlet states that contribute to *D* are reported. ^b*T* is a triplet state, ^c*S* is a singlet state.

In order to rationalize the nature of the contributions, we examined the composition of the wave functions of the ground state and the first four excited triplet states and the three singlet states that contribute to *D*. Table 1 reports the coefficients of the wavefunctions on the determinants expressed in the basis of the cartesian orbitals in the magnetic axes frame. The first observation is that all wavefunctions are highly multideterminantal in this basis. One should note that in its state specific orbitals set, the triplet ground state is strongly monodeterminantal (largest coefficient 0.9996!). Due to the multideterminantal nature of the wavefunctions in the magnetic axes frame, the interpretation of the nature of the contributions to *D* appears to be more complex than in many previously studied cases.[19,21,32] Indeed, we have shown in the past that the sign of the contribution to *D* of each excited triplet

state can easily be explained knowing that an excitation involving orbitals with the same angular momentum component M_l contributes negatively to D , while an excitation involving a change of M_l by ± 1 contributes positively to D .^[19] The sign is opposite when the excited state is a singlet. Using perturbation theory, it is possible to estimate the second-order energy correction of the various M_S components of the ground state due to SOC using the expression :

$$E^{(2)} = \frac{\langle T_0, M_S | \sum_i \zeta_i \hat{l}_i \hat{s}_i | A^*, M_{S'} \rangle}{E_{T_0} - E_{A^*}} \quad (4)$$

where $|T_0, M_S \rangle$ and $|A^*, M_{S'} \rangle$ are the M_S ($M_{S'}$) components of the ground and excited states respectively and E_{T_0} and E_{A^*} their electronic energy. Focusing on the main (largest coefficients) determinants of the ground and excited states is usually enough to rationalize the sign of D and its magnitude. Such a simple reasoning enabled us to find easy ways to tune the D parameter playing on the denominator of equation (4). Indeed, the ligand field theory allows one to relate the nature of the ligand (either weak or strong field) with the relative energy of ground and excited states. Nevertheless, when the wavefunctions are multideterminantal, the numerator of equation (4) is a weighted sum of spin-orbit interactions between the determinants involved in the ground ($|T_0, M_S \rangle$) and excited states ($|A^*, M_{S'} \rangle$). While the sign of the contribution of each excitation taken separately is still governed by the nature of the excitation (either $\hat{l}_z \hat{s}_z$ between same M_l or $\hat{l}_+ \hat{s}_-$ for a change of M_l by ± 1), their sum weighed by the products of the determinants coefficients is affected by the phases of the wavefunctions, i.e. by the sign of the various coefficients. As a consequence, even if the most important determinants of a wavefunction would all generate separately a positive contribution, the weighted sum in the overall SOC between two states M_S components may happen to be close to zero. This can lead to an overall negligible contribution of this state whatever its energy is. In order to illustrate the previous reasoning and to rationalize the contributions to D , the overall couplings (off-diagonal elements of the SO-SI matrix) between the M_S components of the excited states and those of the ground state have been reported in Table 1. The SOC between the three components of the ground state and those of both an excited triplet and an excited singlet states are materialized by arrows in Scheme 2.



Scheme 2. Coupling scheme between the M_S components of the excited triplet (left) and singlet (right) states with the ground triplet state, the continuous and dashed arrows indicate coupling leading to negative and positive D contributions respectively.

Combining all information reported in table 1, one may conclude that both negative and positive contributions are brought by the three first excited triplet states of comparable energy. Indeed, in D_{3d} symmetry point group, the four orbitals (x^2-y^2,xy) and (xz,yz) belong to the same IRREP E_g and can, therefore, be mixed. This mixing is reflected in the structure of the ground state wave function that have contribution of about 18% and 14% of the $|x^2 - y^2, xz|$ and the $|yz, xy|$ determinants in addition to the main one $|yz, xz|$ that contributes to 50%. As a consequence, the ground state can be coupled to the three first excited triplet states using both $\hat{l}_z \hat{s}_z$ and $\hat{l}_+ \hat{s}_-$ operators. For instance, the excitation from x^2-y^2 to xz orbitals couples through $\hat{l}_+ \hat{s}_-$ the $|yz, xz|$ and the $||yz, x^2 - y^2|$ determinants with a change of M_l by ± 1 , it has therefore a positive contribution to D . On the other hand, the excitation from yz to the xz orbitals through $\hat{l}_z \hat{s}_z$ keeps the same value of M_l and contributes negatively to D . Let us now consider the SOC between the various M_S components of the ground state with those of the three excited triplet ones. Let us consider the first excited triplet state: the $M_S = 0$ component of the ground $|T0,0\rangle$ benefits from the two large couplings with the $M_S = \pm 1$ components $|T1, \pm 1\rangle$ of the excited state while the $M_S = \pm 1$ component $|T0,1\rangle$ only benefits from one coupling with the $|T1,0\rangle$ and a much smaller coupling with the $|T1,1\rangle$ (Scheme 2). In summary the overall contribution of $T1$ is positive and large. Concerning the second triplet: while the two couplings between $|T2, \pm 1\rangle$ and $|T0,0\rangle$ are of the same order of magnitude than for $T1$, the couplings between the $M_S = \pm 1$ components between $T2$ and $T0$ are now much larger generating a larger negative contribution to D . Hence, the overall contribution to D is much smaller for $T2$. Concerning the third excited state, one sees a very large coupling between the $M_S = \pm 1$ components between this state and the ground one and a decrease in the couplings that stabilizes the $M_S = 0$ component of the ground state, the contribution is therefore negative. Finally, these couplings are negligible for the fourth triplet states, leading to an almost zero value of its contribution.

Despite their high energy, singlet states have non negligible contributions to D . Looking at the SO-SI elements, it appears that the couplings stabilizing the $|T0, \pm 1\rangle$ are much larger than those stabilizing $|T0,0\rangle$ for the first two states ($S2$ and $S3$ in Table 1). Their contribution is therefore negative. The opposite occurs for the third singlet ($S4$) for which the SOC between the $M_S = 0$ components of ground and excited states is very large, resulting in a large positive contribution to D . The overall contribution of the singlet excited states is negligible as it was quite often observed in Ni(II) complexes.

In conclusion, the D value obtained from calculations is the result of positive and negative contributions of the three excited triplet states that add together to lead to a rather small positive D value. This analysis shows that it is very difficult to predict the sign of D for such a complex. A slight change in the geometry may affect the

contribution to D of the excited states and increase or decrease (in absolute value) the magnitude of the contribution that may result in negative or positive D value. In other words, because of the mixing of the (xz, yz) and (xy, x^2-y^2) sets of orbitals in the D_{3d} symmetry point group, D is expected to be small and its sign difficult to predict. As expected from the quasi axial symmetry of **1**, the principal axis (Z) of the \mathbf{D} tensor is along the pseudo three fold axis of the complex as depicted in Figure 6.

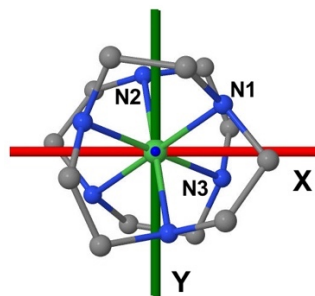


Figure 6. Schematic view of the \mathbf{D} tensor axes with hard axis (Z) along the pseudo three fold axis of the complex (perpendicular), X (horizontal, red) and Y (vertical, green) are the easy and intermediate magnetization axes respectively.

The trigonal geometry of **1** allows us to examine the effect of symmetry and in the present case also geometry on the magnitude and nature of ZFS. To do so, we carried out calculations on model complexes derived from **1** by varying the twist angle Φ (see Scheme 1) from 60 to 0 degree (close to D_{3h}) that corresponds to a geometry very close to prismatic. Calculations were performed for $\Phi = 60, 45, 30, 15$ and 0 degrees.[33] The results (Table 2) show that D remains positive and increases from 4.26 to 73.6 cm^{-1} upon reducing the twist angle. The rhombic parameter remains very weak and $|E/D|$ decreases by one order of magnitude from 0.047 to 0.004.

Table 2. Axial (D) and rhombic (E) parameters as a function of the twist angle Φ .

Φ ($^\circ$)	D (cm^{-1})	E (cm^{-1})	E/D
complex 1 (60)	4.26	0.2	0.047
45	5.83	0.15	0.026
30	12.7	0.24	0.019
15	34.4	0.20	0.006
0	73.6	0.30	0.004

In order to analyse these results and to compare them to those of complex **1**, let us first look at the electronic spectra of these model complexes along the deformation (Fig. 7a). The variation of the energy of the triplet and singlet states contributing to D is depicted in Figure 7, where we observe a decrease of the energy separation between the ground and excited states that may be correlated with the energy of the molecular orbitals (MOs) (Fig

7b) determined by Ab Initio Ligand Field Theory (AILFT). This result is of course in part at the origin of the overall increase of D as contributions of excited states are roughly inversely proportional to these energy differences (see eq. 3). A close examination of the contribution of the different states (Table 1) reveals two main features apart from the variation of the energy separation. We will focus on the comparison between the two extreme cases $\Phi = 60^\circ$ and 0° (Table 1 and Fig. 7).

For $\Phi = 0^\circ$ that corresponds to a symmetry close to D_{3h} , the two sets of orbitals (xy, x^2-y^2) and (xz, yz) belong to two different IRREP E' and E'' , these orbitals cannot mix anymore and for $\Phi = 60^\circ$ (Table 3). As a consequence, the ground triplet state is mainly mono-determinantal, it has contribution of 92% of $|yz, xz|$ and more importantly it does have contributions from the $|x^2 - y^2, xz|$ and the $|yz, xy|$ determinants as for the ground triplet of **1**. Therefore, the SOC between the ground and excited triplet states cannot involve the $\hat{l}_z \hat{s}_z$ operator anymore but only $\hat{l}_+ \hat{s}_-$, i.e. all excited triplet electronic state have a single positive contribution to D . Looking at the SO-SI elements in Table 1, one may observe that the four triplets have now a positive contribution to D as they only interact through $\hat{l}_+ \hat{s}_-$. The values of the overall SOC couplings are very small for the two first ones and very large for the two last ones, rationalizing the two small and two large contributions to D from these triplet states respectively.

While the sum of the contributions of the three singlet states (S_2 , S_3 and S_4) amounted to almost zero for **1** ($\Phi = 60^\circ$), their overall contribution is positive (around 11 cm^{-1}) for $\Phi = 0^\circ$. The wavefunctions of the two first singlet states clearly show that they can only be coupled to the ground state through $\hat{l}_+ \hat{s}_-$ (generating a negative value for a SOC), the last singlet (S_4) can only be coupled through $\hat{l}_z \hat{s}_z$, generating a positive contribution (22.82 cm^{-1}). The very large SO-SI matrix elements coupling the $M_S = 0$ components of the triplet ground state with that of the singlet rationalizes the very important contribution of this state despite its high energy. One could note that such an important overall contribution of excited singlet states is quite unusual in Ni(II) hexacoordinate complexes and is probably due to the close to D_{3h} symmetry of the model complex.

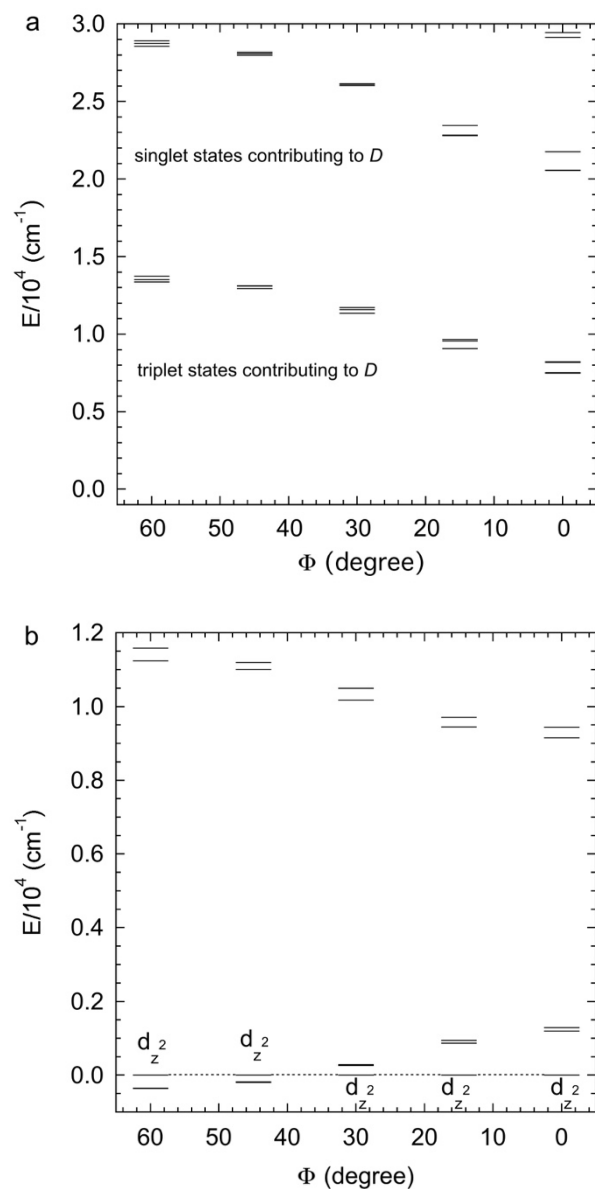


Figure 7: Energy of the excited states contributing to D (a) and of AILFT molecular orbitals (b) obtained for **1** ($\Phi = 60^\circ$) and model complexes as a function of the twist angle, see Table 3 for the composition of the MOs as a function of Φ .

Table 3. Pure d orbitals and MOs AILFT (CASSCF level) energy (in cm $^{-1}$) as a function of the twist angle Φ and composition of the AILFT MOs for **1** and $\Phi = 0^\circ$

1 (60°)			45°		30°		15°		0°		
pure ^a	AILFT CASSCF	composition of the AILFT MO	pure ^a	AILFT CASSCF	composition of the AILFT MO						
0	0	-0.41xy + 0.54yz - 0.73(x ² -y ²)	0	0	0	0	0	0	0	0	z ²

1898	-390	0.99z ²	1828	-254	1466	126	1061	580	885	804	0.93xy - 0.38(x ² -y ²)
2066	-373	-0.76xy + 0.46yz + 0.45(x ² -y ²)	1891	-227	1510	170	1132	655	968	893	-0.38xy + 0.93(x ² -y ²)
6867	9071	-0.37xy + 0.2yz - 0.86xz + 0.27(x ² -y ²)	7306	8915	7557	8260	7888	7622	8109	7307	-0.66yz - 0.76xz
7390	9422	-0.33xy - 0.82yz - 0.17xz - 0.43(x ² -y ²)	7378	9109	7725	8559	8070	7845	8156	7539	-0.76yz + 0.66xz

^apure orbitals at CASSCF level in the magnetic axes basis frame

4. Conclusion

In conclusion, the parameters extracted from the HF-HFEPR spectra are in very good agreement with those obtained from field-dependent powder magnetization. HF-HFEPR yields more precise values and above all enables discriminating between the two sets of parameters (negative and positive D) obtained from magnetization measurements, indicating that **1** has an easy plane anisotropy. Wave function based calculations reproduce fairly well the magnitude of D and E and more importantly the sign of the axial parameter. The relatively small D value of **1** is due to its octahedral geometry where orbital mixing is responsible for the simultaneous appearance of positive and negative contributions from the same excited state leading to positive and negative contributions to D of the different states that when they add lead to weak overall D value. This phenomenon makes it difficult to estimate the contributions using simple chemical considerations such as the ligand field theory as each state may generate contributions of opposite signs. Furthermore, the estimation of a SOC between two multiconfigurational states is complex because it is a sum of interactions weighted by products of determinant coefficients whose signs can lead to a (quasi) cancellation of the resulting term. Even when the sign of the contribution is well defined, the amplitude of the resulting coupling can be difficult to predict without *ab initio* calculations. This is why weak and large contributions to D were observed for triplet excited states that have almost the same energy separation with the ground state. For D_{3h} symmetry and therefore prismatic geometry, because of the absence of orbital mixing, the energy separation between the ground and the excited triplet states is reduced (from an average of 13500 to 7700 cm⁻¹ leading to an increase of 75% of the contributions to D) and the contribution of the triplet states are *all positive* and therefore add together. These two complementary effects both contribute to increase D from 4 to 73

cm⁻¹ when the geometry changes from octahedral (close to D_{3d} symmetry) to prismatic (D_{3h} symmetry). In order to test this theoretical prediction, we plan to experimentally investigate the EPR of two Ni(II) complexes already reported and that have a geometry very close to prismatic.[34,35]

Acknowledgments

We thank the CNRS (Centre National de la Recherche Scientifique), the Université Paris-Saclay for financial support. We also thank H. Weihe for provision of the EPR simulation softwares.

The authors declare no conflicts of interest

5. References

- [1] A. Abragam and B. Bleaney, *Electron Paramagnetic Resonance of Transition metal Ions*, (Dover Publications, New York, 1970), pp. 449-455.
- [2] F. E. Mabbs and D. Collison, *Electron Paramagnetic Resonance of d Transition Metal Compounds*, (Elsevier, Amsterdam, 1992).
- [3] D. Gatteschi and L. Sorace, *J Sol. St. Chem.* 159, 253 (2001).
- [4] J. Mroziński, A. Skorupa, A. Pochaba, Y. Dromzée, M. Verdagner, E. Goovaerts, H. Varcammen, and B. Korybut-Daszkiewicz, *Journal of Molecular Structure* 559, 107 (2001).
- [5] J. Krzystek, J.-H. Park, M. W. Meisel, M. A. Hitchman, H. Stratemeier, L.-C. Brunel, and J. Telser, *Inorg. Chem.* 41, 4478 (2002).
- [6] G. Rogez, J. N. Rebilly, A. L. Barra, L. Sorace, G. Blondin, N. Kirchner, M. Duran, J. van Slageren, S. Parsons, L. Ricard, A. Marvilliers, and T. Mallah, *Angew. Chem. Int. Ed.* 44, 1876 (2005).
- [7] P. J. Desrochers, J. Telser, S. A. Zvyagin, A. Ozarowski, J. Krzystek, and D. A. Vicic, *Inorg. Chem.* 45, 8930 (2006).
- [8] J. N. Rebilly, G. Charron, E. Riviere, R. Guillot, A. L. Barra, M. D. Serrano, J. van Slageren, and T. Mallah, *Chem. Eur. J.* 14, 1169 (2008).
- [9] R. Ruamps, R. Maurice, L. Batchelor, M. Boggio-Pasqua, R. Guillot, A. L. Barra, J. J. Liu, E. Bendeif, S. Pillet, S. Hill, T. Mallah, and N. Guihery, *J. Am. Chem. Soc.* 135, 3017 (2013).
- [10] D. Schweinfurth, J. Krzystek, I. Schapiro, S. Demeshko, J. Klein, J. Telser, A. Ozarowski, C. Y. Su, F. Meyer, M. Atanasov, F. Neese, and B. Sarkar, *Inorg. Chem.* 52, 6880 (2013).
- [11] K. E. R. Marriott, L. Bhaskaran, C. Wilson, M. Medarde, S. T. Ochsenein, S. Hill, and M. Murrie, *Chem. Sci.* 6, 6823 (2015).
- [12] G. Charron, E. Malkin, G. Rogez, L. J. Batchelor, S. Mazerat, R. Guillot, N. Guihery, A. L. Barra, T. Mallah, and H. Bolvin, *Chem. Eur. J.* 22, 16848 (2016).
- [13] R. Yang and L. J. Zompa, *Inorg. Chem.* 15, 1499 (1976).
- [14] R. Stranger, S. C. Wallis, L. R. Gahan, C. H. L. Kennard, and K. A. Byriel, *J. Chem. Soc. Dalton Trans.*, 2971 (1992).
- [15] A.-L. Barra, L.-C. Brunel, and J. B. Robert, *Chem. Phys. Lett.* 165, 107 (1990).
- [16] S. Mossin, H. Weihe, and A. L. Barra, *J. Am. Chem. Soc.* 124, 8764 (2002).
- [17] J. Glerup and H. Weihe, *Acta Chem. Scand.* 45, 444 (1991).
- [18] R. Maurice, R. Bastardis, C. d. Graaf, N. Suaud, T. Mallah, and N. Guihéry, *J. Chem. Th. Comput.* 5, 2977 (2009).
- [19] R. Ruamps, L. J. Batchelor, R. Maurice, N. Gogoi, P. Jimenez-Lozano, N. Guihery, C. de Graaf, A. L. Barra, J. P. Sutter, and T. Mallah, *Chem. Eur. J.* 19, 950 (2013).
- [20] F. Shao, B. Cahier, N. Guihéry, E. Rivière, R. Guillot, A.-L. Barra, Y. Lan, W. Wernsdorfer, V. E. Campbell, and T. Mallah, *Chem. Commun.* 51, 16475 (2015).
- [21] F. El-Khatib, B. Cahier, M. López-Jordà, R. Guillot, E. Rivière, H. Hafez, Z. Saad, J.-J. Girerd, N. Guihéry, and T. Mallah, *Inorg. Chem.* 56, 10655 (2017).
- [22] C. Angeli, R. Cimraglia, S. Evangelisti, T. Leininger, and J. P. Malrieu, *J. Chem. Phys.* 114, 10252 (2001).
- [23] C. Angeli, R. Cimraglia, and J.-P. Malrieu, *Chem. Phys. Lett.* 350, 297 (2001).
- [24] C. Angeli, R. Cimraglia, and J.-P. Malrieu, *J. Chem. Phys.* 117, 9138 (2002).
- [25] F. Neese, *J. Chem. Phys.* 122, 034107 (2005).

- [26] G. L. Stoychev, A. A. Auer, and F. Neese, *J. Chem. Th. Comput.* 13, 554 (2017).
- [27] F. Neese, *J. Comput. Chem.* 24, 1740 (2003).
- [28] M. Reiher, *Theor. Chem. Acc.* 116, 241 (2006).
- [29] F. Neese, *Wiley interdisciplinary Reviews -Computational Molecular Science* 2, 73 (2012).
- [30] A. Bencini and D. Gatteschi, *Transition Metal Chemistry*, Dekker, New York, 1982), Vol. 8, pp. 1-178.
- [31] D. Collison, M. Helliwell, V. M. Jones, F. E. Mabbs, E. J. L. McInnes, P. C. Riedi, G. M. Smith, R. G. Pritchard, and W. I. Cross, *Journal of the Chemical Society, Faraday Transactions* 94, 3019 (1998).
- [32] B. Cahier, M. Perfetti, G. Zakhia, D. Naoufal, F. El-Khatib, R. Guillot, E. Riviere, R. Sessoli, A. L. Barra, N. Guihery, and T. Mallah, *Chem. Eur. J.* 23, 3648 (2017).
- [33] It is worth noting that the model complex with $\Phi = 60^\circ$ obtained by turning the twist angle of **1** by 120° keeps the pseudo D_{3d} symmetry as complex **1**. We checked that the ZFS parameters of the as obtained model ($\Phi = 60^\circ$) are almost identical ($D = 4.2 \text{ cm}^{-1}$, $E = 0.16 \text{ cm}^{-1}$ and $E/D = 0.037$) to those of **1**, suggesting that (i) loosing the inversion symmetry does not affect the ZFS parameters and (ii) the model complex with $\Phi = 60^\circ$ is a reasonable model for **1**. For ($\Phi = 0^\circ$), the model complex has a σ_h symmetry plane.
- [34] M. R. Churchill and A. H. Reis, *J. Chem. Soc. D: Chem. Commun.*, 879 (1970).
- [35] S. Ross, T. Weyhermüller, E. Bill, K. Wieghardt, and P. Chaudhuri, *Inorg. Chem.* 40, 6656 (2001).